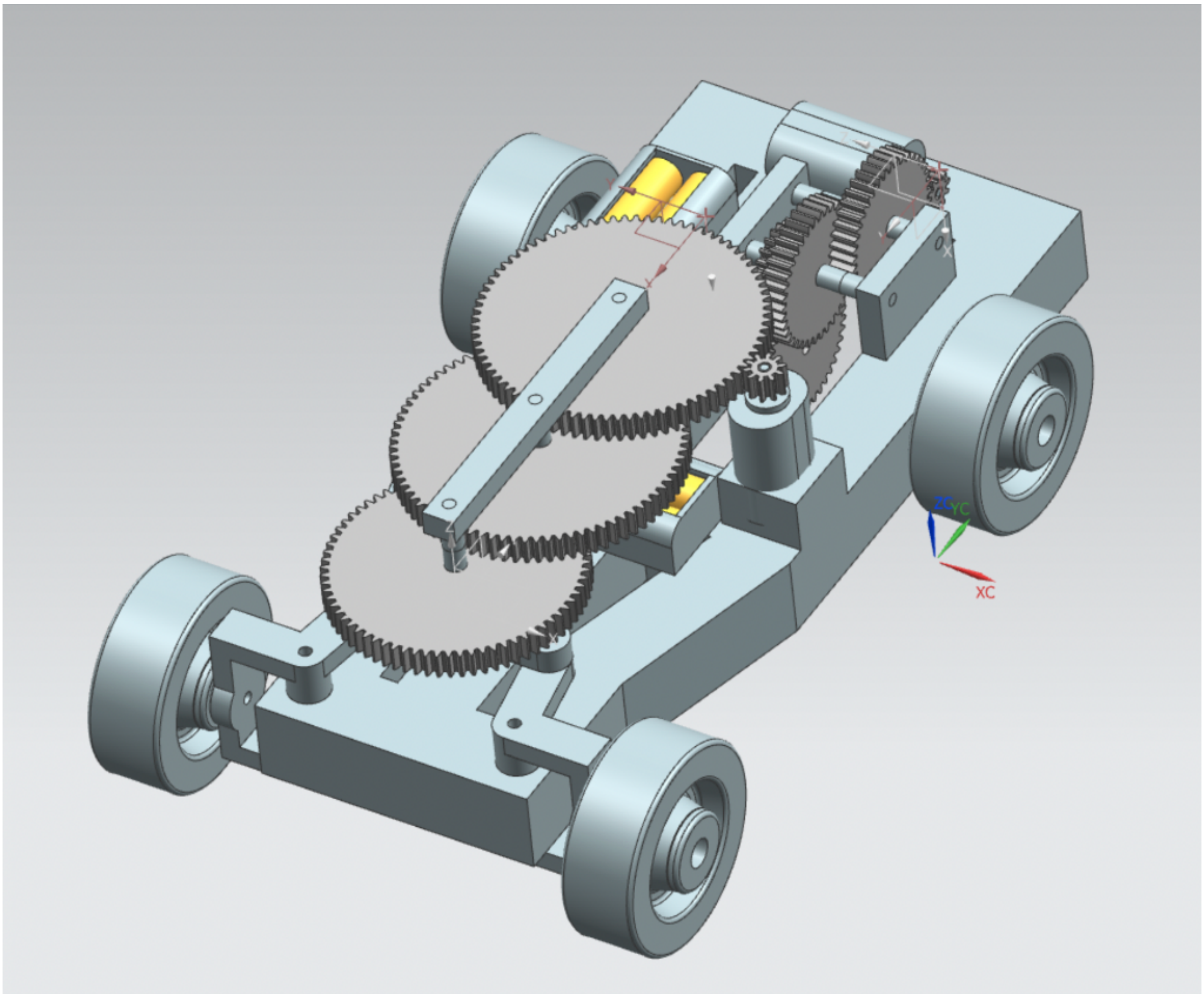

Group A Project.

Student IDs: F122967, F126225, F132621, F127992, F015746

Module: TTA207 – Vehicle Systems and Design

Module Tutor: Scot Layton

Date: 12/04/2022

Word Count: 2464

Contents

1.0. Introduction

Our aim is to prove our company's automated vehicle deserves large scale production, through testing a prototype in a 5-meter slalom and 20-degree inclined ramp in 60 seconds.

Our company has been divided into five teams, ain a flat structure, joined by a group leader to promote communication and structure workload. Using Gantt chart to track progress and ensure we completed tasks on time. We initially manged to meet the optimistic deadlines set, but as the tasks grew more challenging, we had to readapt to accommodate these larger problems. This evolution was facilitated by initially setting the challenging goal of completing the project before the Easter break as it ensured we had time to adapt our schedule depending on workload.

Project Planner

Select a period to highlight at right. A legend describing the charting follows. Period Highlight: 1 Plan Duration Actual Start % Complete Actual (beyond plan) % Complete (beyond plai

ACTIVITY	PLAN START	PLAN DURATION	ACTUAL START	ACTUAL DURATION	PERCENT COMPLETE
Assign Job Roles	1	1	1	1	100%
Define Project Goals	2	2	1	3	100%
Measure Parameters	2	2	2	2	100%
Access data required	2	2	2	4	100%
Ascertain constraints	2	2	2	4	100%
Steering concept	3	2	2	1	100%
Powertrain concept	3	2	3	2	100%
Chassis concept	3	2	4	2	100%
Upright concept	3	2	4	2	100%
Gear calcs	3	2	5	3	100%
Steering calcs	3	2	5	3	100%
Powertrain calcs	3	2	5	2	100%
Steering design sign off	5	2	8	1	100%
Powertrain design sign off	5	2	8	1	100%
Upright design sign off	5	2	6	1	100%
Chassis design sign off	5	2	8	2	100%
Gear design sign off	5	2	8	1	100%
CAD Assembly	7	2	8	2	100%
Project Write Up	7	2	9	2	100%
Presentation	7	2	9	2	100%

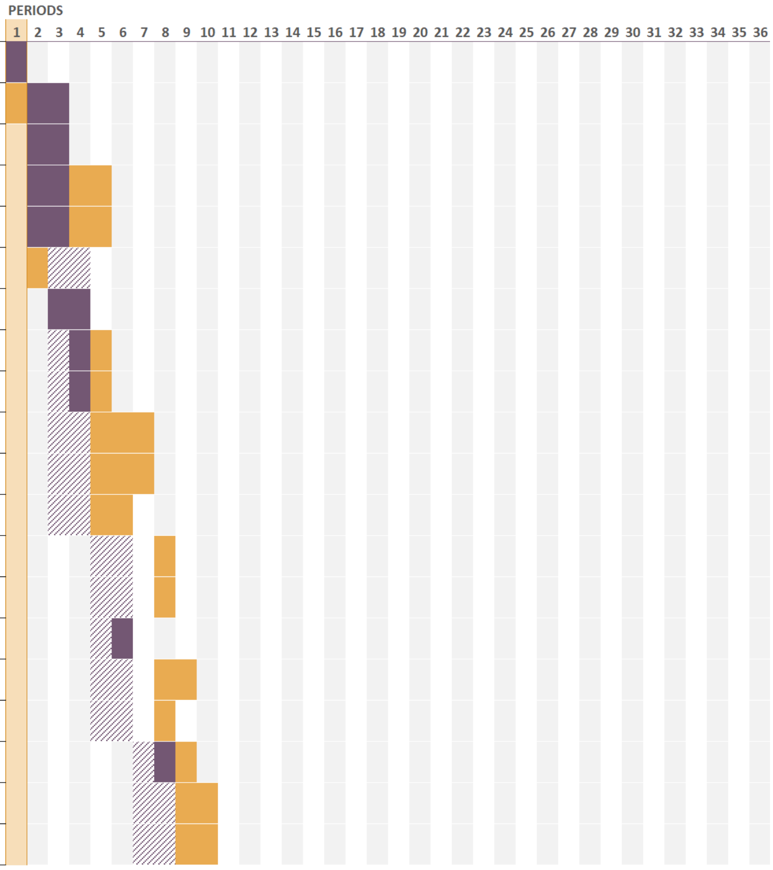

Table 1: Gannt Chart displaying the progress of the project

2.0. Simulation - (F127992)

2.1 Modelling the Ramp Test

Before designing any components, we need to establish constraining factors on the vehicles track width and wheelbase, as these would be used to determine the size, shape, and action of all further systems. Following analysis of the project brief we determined that the slope test would limit these critical elements.

As the ramp is only 250mm wide, it's critical to maintain a considerable clearance either side of the vehicle to ensure that any discrepancies in the vehicle's path would not result in it falling off. A smaller track would additionally reduce weight and consequently improve performance for the Hillclimb. Therefore, we decided a track of 120mm would be wide enough to accommodate the onboard components, while maintaining a margin of error of 65mm either side.

An excessive wheelbase would cause the vehicle to beach when going over the peak of the slope and so we developed an approximate model to analyse the motion of the vehicle during the test.

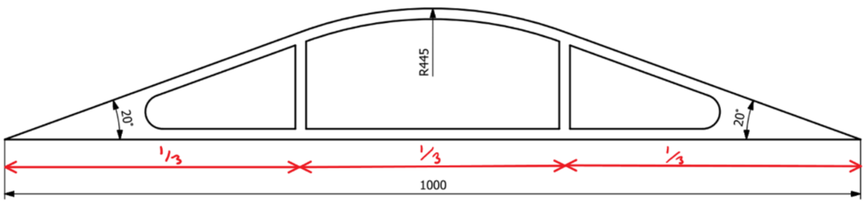

Figure 1: annotated ramp diagram

It can be deduced from inspection that each section consists of one third of the overall length. As the curved peak would be the limiting factor on wheelbase, this facilitated further analysis.

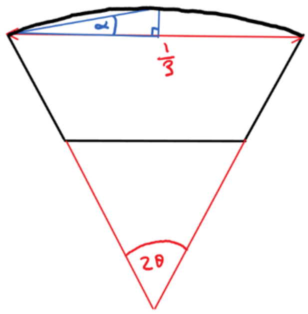

Figure 2: expanded diagram of curved ramp section

Approximating the curved surface of the peak to be straight with inclination alpha (a reasonable assumption given alpha is small) allowed the angle of inclination to be calculated through trigonometric ratios.

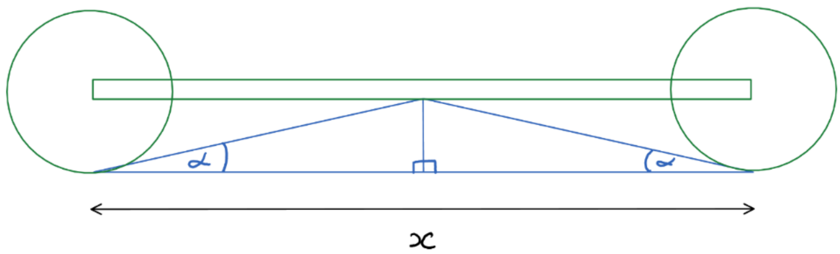

Figure 3: approximate model of the car travelling over the peak of the ramp to find maximum wheelbase

Using the inclination of the curve and the vehicle clearance (given by the radius of the wheel minus half of the thickness of the chassis material), the maximum wheelbase (x) could be calculated. This gave a value of 154 mm and so we concluded a wheelbase of 150mm was suitable.

2.1 Modelling the Slalom Test

When considering the slalom test, we concluded that it would be beneficial to create a graphical representation of the vehicles path in Matlab to help conceptualise the steering system.

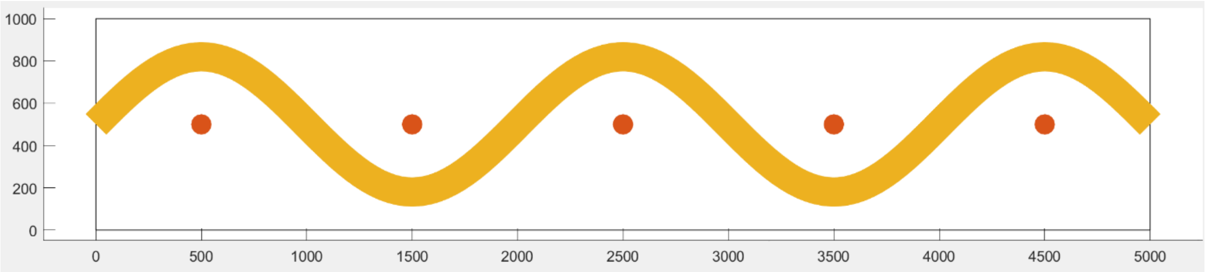

Figure 4: simulation model of the vehicle's path around the slalom course

From modelling different paths onto this graphing template, it was decided that the tightest turn radius of the inside wheel should be 320mm. This path was narrow enough to not necessitate an excessive steering angle and allowed the vehicle to remain distant from both the outer boundary and the central cones. This minimised the possibility of collision/exit from area due to tolerancing issues or errors. Calculating the maximum turn radius facilitated the calculation of the steering angles and the development of the steering system.

3.0. Drivetrain - (F015746) (F126225)

3.1 Maths

We started the design of the drive train by estimating the maximum weight of the vehicle so that we could evaluate the torque our drive train needed to produce for the rear wheels. We will not end up using all the materials provided but this will ensure that the vehicle will be able to climb the ramp.

We estimated the maximum weight by researching the parts and making suitable assumptions for the materials used for the vehicle. We concluded the maximum weight for the vehicle to be 390 grams. We found the weight parallel to the slope to be 1.31 Newtons, a torque of 0.0327 Nm (333 g-cm) would have to be produced at the 50mm diameter wheels to overcome this. We assumed the rolling resistance at the wheels is negligible and that the torque does not split at the wheels. This also provided us with an rpm of 386.9, giving a vehicle speed of 1.01 meters per second.

3.2 Gear Concepts

We used one of the two motors to power vertical gears for the drive train. "Motor Data" showed that the motor would have a torque of 10.5 g-cm at 3.0V (two AA batteries). To achieve the 333 g-cm, we used a compound gear system with gear ratios of 4:1, 4:1, 2:1, respectively. A compound gear gives a larger gear ratio than a simple gear train for the same length.

The drivetrain system had to increase torque whilst using minimum space, to ensure it will fit on the chassis, and the final gear to exceed 50mm (wheel diameter). We initially designed gears with modules of 0.4 and 0.3 with a 3mm inner diameter for the gear axle and 2mm for the gear that will be press fit onto the motor. The problem with this was how close the teeth were to each other and without knowing the accuracy the laser we did not know if the result will be as detailed. So, we increased the module to 0.8 and decrease the number of teeth.

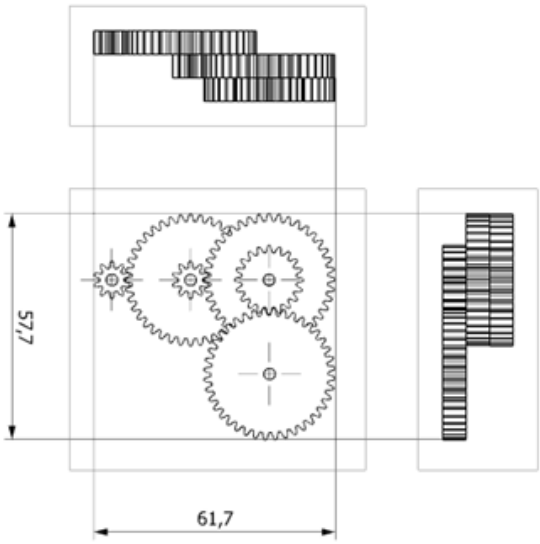

Figure 5: Orthographic drawing of drive train gears

3.3 Final Design

The final design consisted of compound gears using the above-mentioned ratios with a module of 0.8 (See Appendix 3.3). The final gear of the system would have the rear axle of the vehicle going through the centre, this would have the 2 rear wheels on the end of the axles making our vehicle RWD, and the turning of the vehicle easier to design. The drive train would be held in place with some lasers cut plywood holding the axles the gear spins on, this would be attached to the chassis.

"Gear spacers" (laser cut circular ply with an outer diameter of 5mm and an inner diameter of 3mm) ensures the gears are spinning in the correct position these are held in place by the gear axles. We used this to distance the gears from the axle holders as it reduces the energy loss as there is less friction compared to if it were to spin against the axle holders.

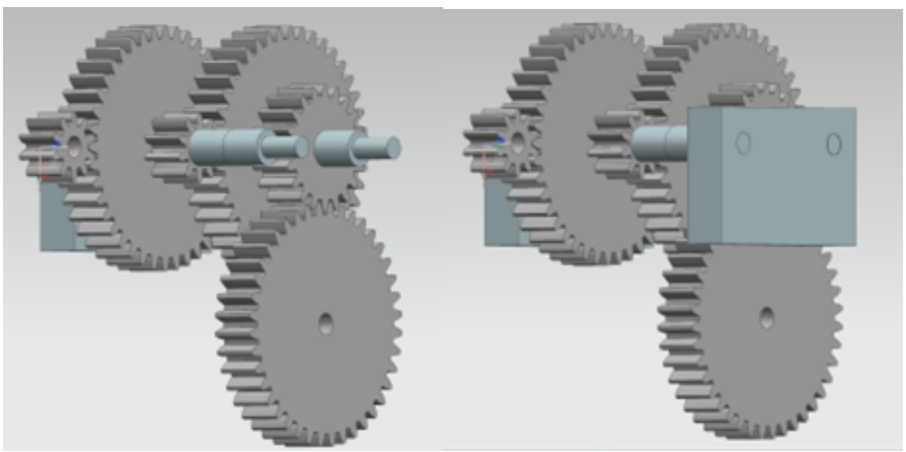

Figure 6: CAD of drive train

4.0. Steering - (F122967) (F127992) (F015746)

4.1 Steering angle calculations

Before undertaking any calculations, we had to conceptualise a mechanism to convert the rotary motion from the motor to the linear motion required to turn the wheels. Following research, we decided the simplest approach was to implement a Scotch Yoke to push the steering rack. This design was chosen as it can easily be laser cut from the provided plywood and its reciprocating motion is much like to that of a conventional steering rack, ensuring more intuitive and simple calculations. It can also be directly attached to a gearing system.

Following the calculation of the wheelbase and the maximum radius of turn it was possible to evaluate the maximum steering angle. This would be used to calculate the size of the Scotch Yoke.

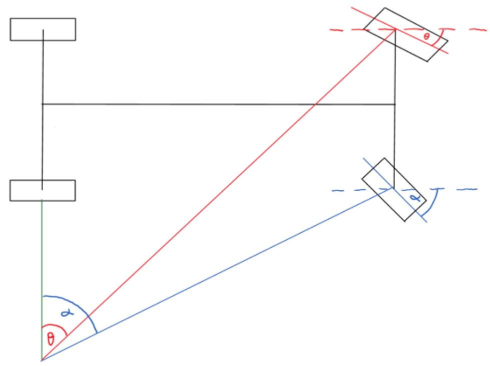

Figure 7: diagram demonstrating steering angles

This diagram shows how the steering angles can be calculated. We only need to consider the steering angle of the inner wheel as the toe out of the outer tyre will be accounted for through implementation of 100 percent Ackerman tie rods as this is the most suitable steering model for low-speed applications (Colgrove, 2019).

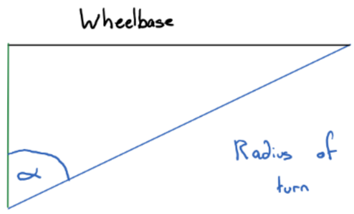

Figure 8: expanded diagram of inside wheel steering angle

Considering the max radius of turn (320mm), use of trigonometric ratios revealed a maximum steering angle of 28.0 degrees (3 S.F) (0.488 Rad).

4.2 Calculating the dimensions of the Steering rack

This maximum steering angle can be applied to models of the steering rack in a normal position and at full outer lock which can be used to evaluate the size of yoke.

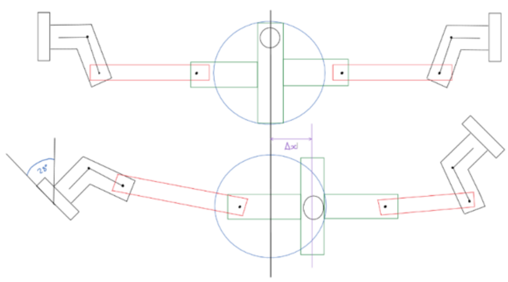

Figure 9: diagram of the steering system in a normal position and at its maximum angle

Upon simplification of the system into members and recognising the constrained vertical distance between the centre of the yoke and the axis of rotation, resolving member lengths in both diagrams vertically and horizontally provided equations which could be solved simultaneously to give delta x. This is equal to the radius of the yoke as shown in figure 7. These equations do require length L and C but as these are not constrained provided L + ½C + 22sin(10) = ½ of the wheelbase. This ensured that L and C could be set arbitrarily.

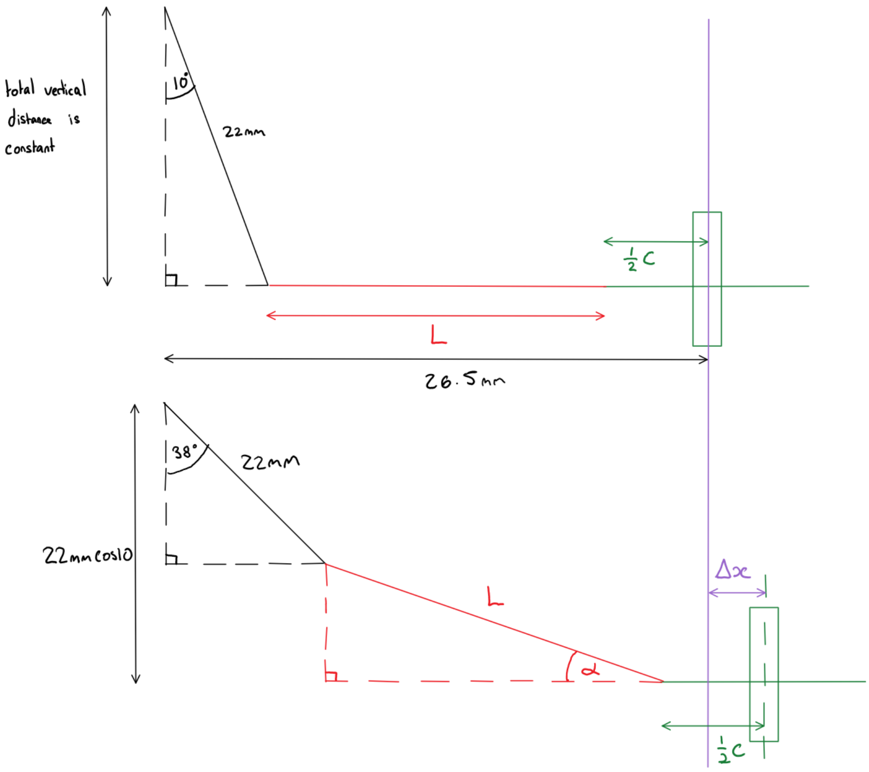

Figure 10: simplified diagram of steering system to determine the size of the central yoke

4.3 Rendering the steering rack into CAD

With the size of all steering rack components determined, it can be modelled in CAD. A guide is also added underneath.

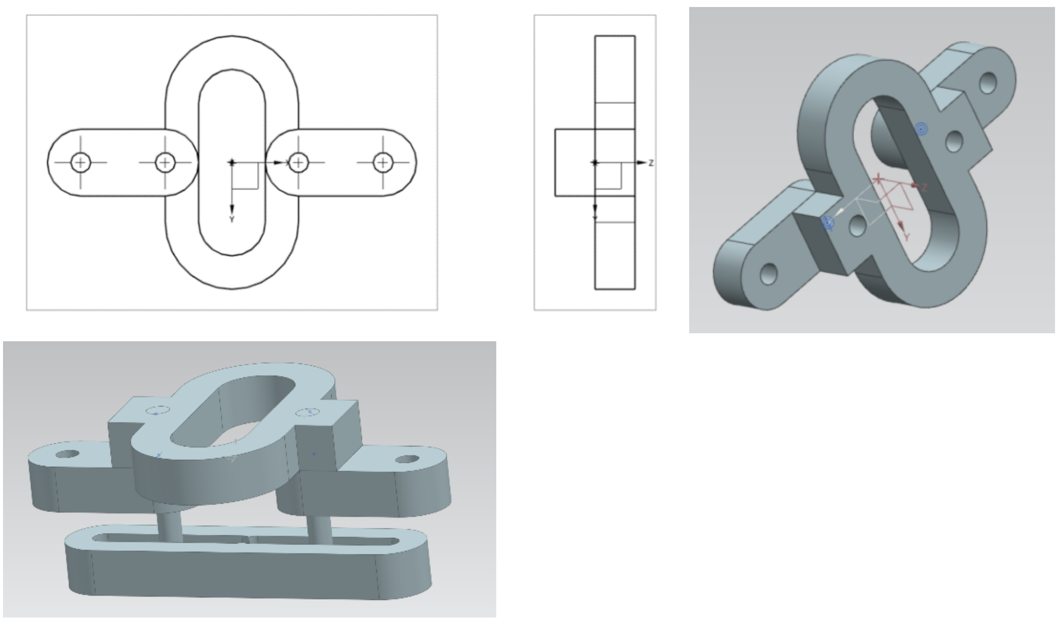

Figure 11: CAD models of the assembled steering rack with and without the guide

4.4 Calculating the rotational frequency of the Scotch yoke

The rotational frequency of the yoke had to be determined to design the gearing system powering it. This required analysis of the rate of change of steering angle achieved through resolving the velocity of the vehicle (which was given by the powertrain analysis to be 1.01 meters per second) horizontally and forming a differential equation.

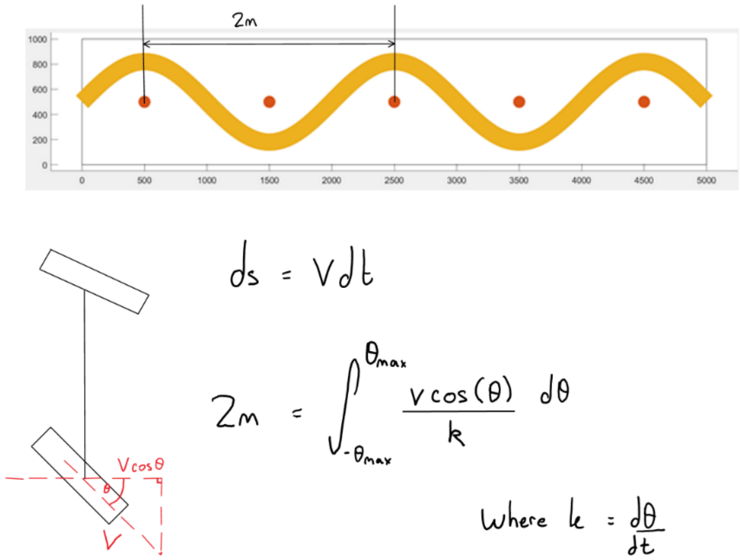

Figure 12: diagrams demonstrating how the differential equation to ascertain the rate of change of steering rack has been formed

Once the rate of change of steering angle had been calculated (0.473 radians per second), the period for one full cycle could further be evaluated (2.06 seconds). The period can then be used to find the rotational frequency of the central yoke (28.2 revolutions per minute).

4.5 Gear System

We used one of the two motors to power horizontal gears for the steering. “Motor Data” showed that the motor would have a rpm of 6500 at 1.5V (one AA battery). The battery pack provided is a two AA battery pack (3.0V), but this would make the motor run at 12,380 rpm. Reducing the rpm of the motor from 12,380 to 29.1 rpm would require a gear ratio of 425.4:1, and would require a long system, which is not ideal as there would be more room for error as there is more mechanical parts to achieve this. We assumed that we could just use one AA battery to power the motor at 6500 rpm with 1.5V of power. Reducing the rpm from 6500 to 29.1 rpm would require a gear ratio of 223.4:1 which is more than half if we were to run it at 3.0V. To achieve the 29.1 rpm, we used a compound gear system with gear ratios of 8:1, 8:1, 3.5:1, respectively. We have called this system the “steering train.”

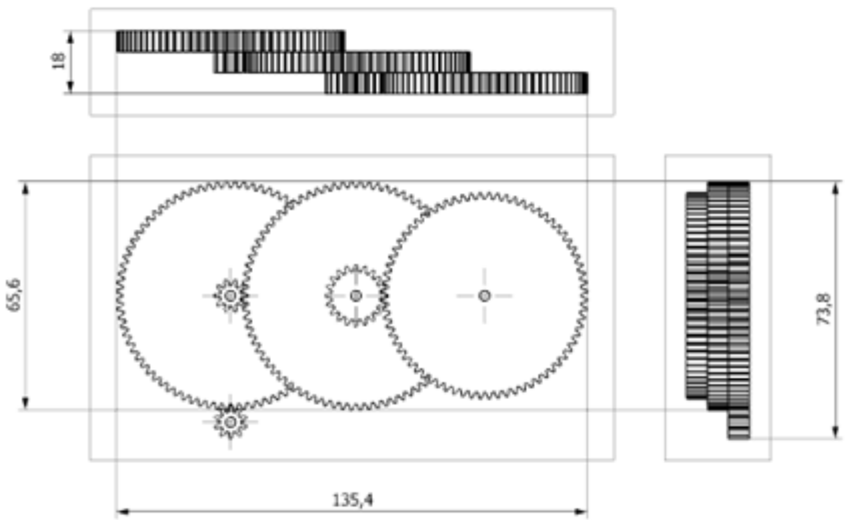

Figure 13: Orthographic drawing of steering train system

The design of the steering train allowed the final gear to spin with the Scotch Yoke spinning on top of it with no obstructions. The steering train would be held in place by axles going through the chassis and laser cut ply.

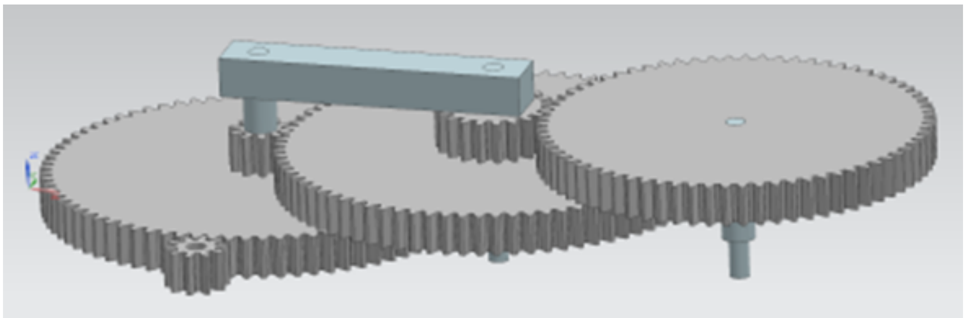

Figure 14: CAD of steering train

4.6 Uprights

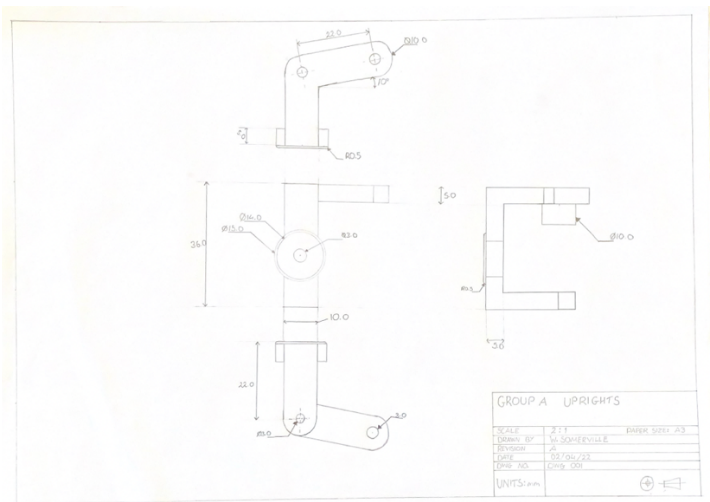

Figure 15: Technical Drawing of final uprights

After research into OEM current uprights in the RC car industry, I settled on a rough design and based my uprights on double wish bone suspension sports cars. With their two-point contact above and below the main body with a steering arm coming from the same area.

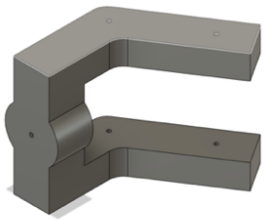

First prototype, a general idea of the design and shape that the upright is going to take. But clearance issues with thickness of the front plate. As well as incorrect Ackermann calculations.

Figure 16: First Prototype of Upright

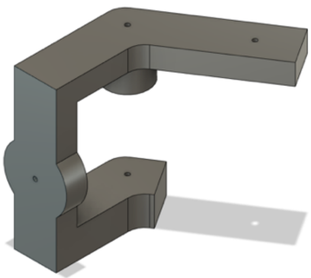

With a better understanding of the fitment and application of the uprights. The front plate shortened to 5mm for clearance. The bottom arm was upgraded so it does not interfere with ground clearance or create unnecessary friction.

Top arm also redesigned with the 3mm axle shaft connection to the steering yoke in mind.

Figure 17: Second Prototype of Upright

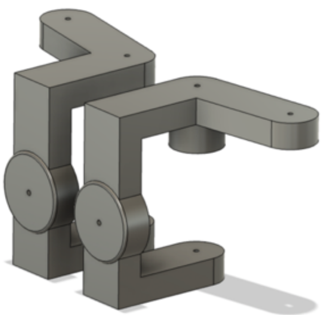

Correct Ackermann calculations implemented. As well as the addition of a lip on the front plate for the wheel to sit on.

Both the lower and upper arms are now rounded off, creating a smooth surface that won't interfere with the chassis

Figure 18: Final design of uprights

5.0. Powertrain - (F015746)

We were provided 2 motors, powered by two AA batteries each. One to power vertical gears for the drivetrain, powered at 3.0V and running at 12380rpm and a torque of 10.5g-cm. The drivetrain will increase motor torque to 336g-cm and decrease rpm to 386.9. Rear placement ensures more traction to the rear wheels.

The second motor, powering horizontal gears for the steering train, runs at 1.5V giving an rpm of 6500 and torque of 6.2g-cm. The steering train decreases the rpm 29.1 and provides torque of 1428.5g-cm. Placed more centrally this distributes the weight well.

6.0. Chassis - (F132621)

6.1 Initial Ideas

Through assessing vehicle requirements against common design methods used in industry, it's easy to break chassis design down into 3 solutions: Monocoque, Spaceframe and Ladder.


Figure 16: Monocoque Chassis

A monocoque chassis doesn't appear to be a viable choice as we don't have a requirement of aerodynamic performance. Also, with our limitation of using only box section, it's an unnecessarily complex design to go with.

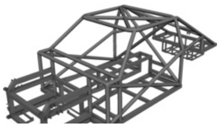
Figure 17: Spaceframe Chassis

The use of a spaceframe isn't necessary as our chassis doesn't need to be able to withstand high forces/stresses. As well, there isn't a need for a roll cage or similar structure due to the tasks.

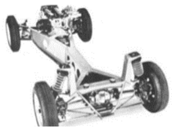
Figure 18: Backbone Chassis

I did consider a backbone chassis from the shape and simplicity. It would provide sufficient steering clearance and strength, but I felt it lacked space to mount components.


Figure 19: Ladder Chassis

Ultimately, I decided to use a ladder chassis as the basis for development. A proven platform that will provide enough strength, rigidity, and mounting points for the necessary components.

6.2 Team input

As decided amongst the team (shown in above calculations), the constraining factors of my design are a track of 120mm and a wheelbase of 150mm, to allow steering system to work and provide adequate ground clearance. Additionally, I need to incorporate both the drivetrain and the steering system while allowing all to work as intended.

This will be achieved using NX and the assemblies provided by both teams.

6.3 Chassis Development

With this in mind and taking inspiration from a classic 4x4 design used by Land Rover, Toyota and many more OEMs, rough sketches were showed to the team (figure 20), and it was decided simplicity is key for success.

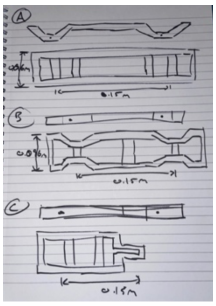
Figure 20: Chassis choices

Option C (Figure 20) was picked as a start point and a preliminary design was drawn up. The conventional design of parallel chassis members with axles suspended beneath was discounted in favour of a design which narrowed at the front to permit the full steering angles to be available.

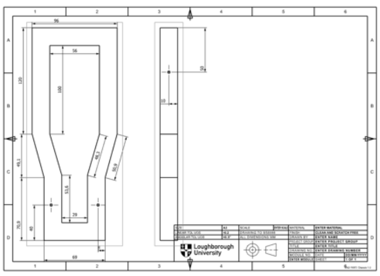
Figure 21: Preliminary Chassis

A rectangular chassis of 240mm long by 96mm wide at rear, narrowing to 69mm wide 169.1mm from the rear; providing required track and wheelbase. The narrowed section allows for a constant track but also the steering clearance. Shown in figure 21.

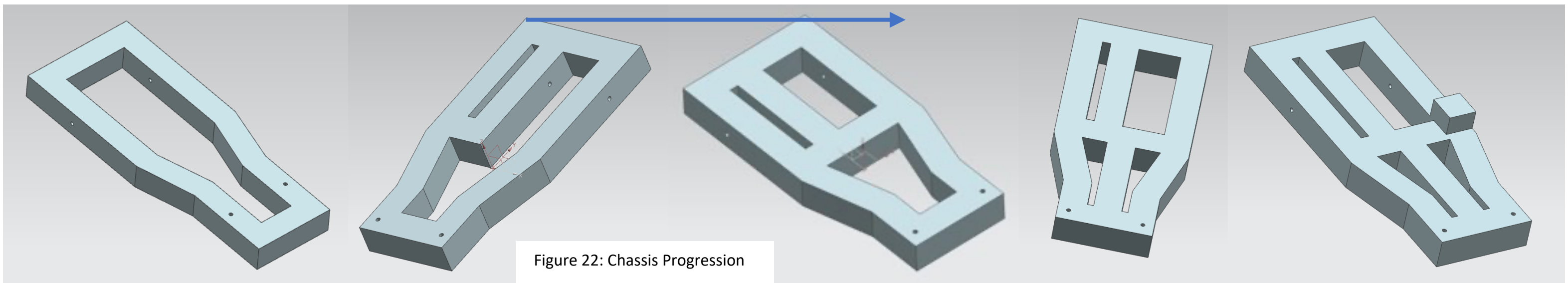

Figure 22: Chassis Progression

Figure 22 is the progression of the chassis design. The preliminary design had larger than required overhangs, due to the uncertainty of fitment of components. The rear drivetrain was first to be culminated into the design, requiring the addition of material for mounting purposes (shown in Figure 23). After the addition of the steering assembly, I decided to eliminate the front overhang and reduce the rear to be able to accept the rear axle and gear. Reduction in material reduces weight and promotes central weight distribution. A central 'rung' was introduced, bracing the structure, and providing more space to mount components etc.

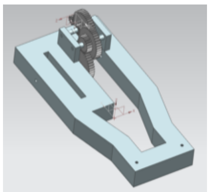

Figure 23: Chassis Progression

Due to the difference between steering components intended use and practical fitment the gear-train is needing to be mounted higher than intended; this will affect the vehicle on the incline however this can be minimised from weight distribution. A central member is added to accommodate 3mm Axle and plywood spacers, used to locate them at the required height.

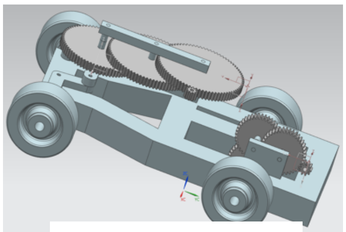

Figure 24: Chassis Progression

Figure 25 is the fully finalised design.

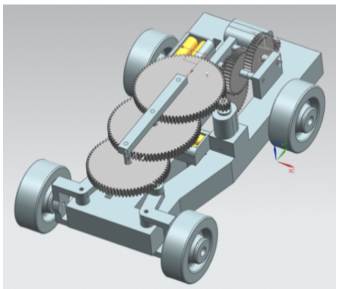

Figure 25: Final CAD Design

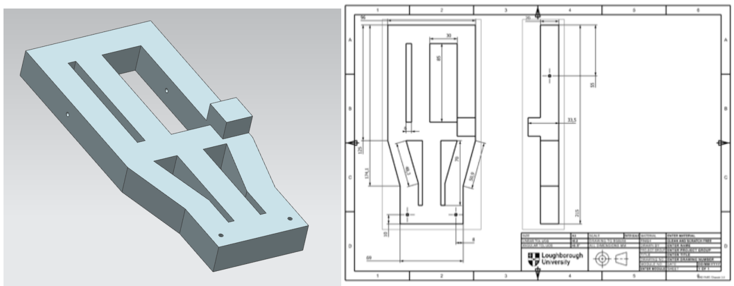

Figure 26: Final Chassis

7.0. Appendix

Appendix for 2.1

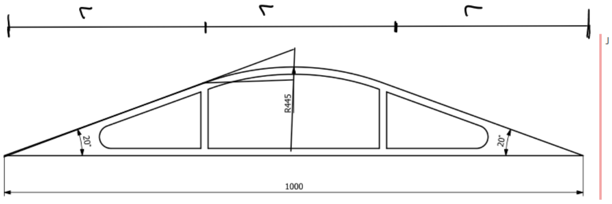

By inspection each section is $\frac{1}{3}$rd

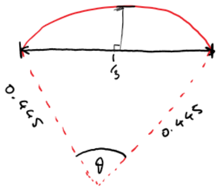

$$\theta = \cos^{-1}\left(\frac{0.445^2 + 0.445^2 - \frac{1}{3}^2}{2 \times 0.445 \times 0.445}\right)$$

$= 44°$

0

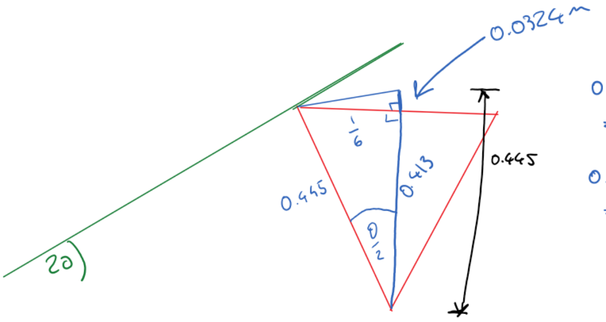

$0.445 \times \cos\frac{\theta}{2}$

$= 0.413$

$0.445 - 0.413$

$= 0.0324$ – this is the max height difference due to the arc

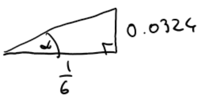

$\alpha = \tan^{-1}\left(\frac{0.0324}{\frac{1}{6}}\right)$

$\alpha = 11°$ – finding angle of incline for arc

ground clearance = 0.015

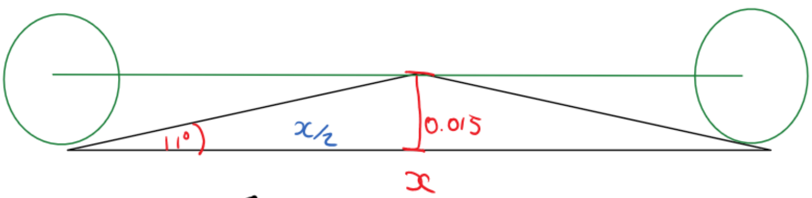

toa

$x/2 = \frac{0.015}{\tan 11°}$

$x = 2 \times \frac{0.015}{\tan(11°)}$

$x = 0.154\ m$

This is a section of the arc, max clearance we have is 0.015m, so max wheelbase is 0.154m

Appendix for 2.2

```
figure(1),clf
hold on
outergrid = [0,0;0,1000;5000,1000;5000,0;0,0];
plot(outergrid(:,1),outergrid(:,2),'k')
axis equal
axis([-250,5250,-50,1050])
cones = [500,500;1500,500;2500,500;3500,500;4500,500];
plot(cones(:,1),cones(:,2),'o','LineWidth',8)
t = [0:0.1:5000]';
path = sin(t*2*pi/2000)*320+500;
plot(t,path,'lineWidth',20)
%open figure in fullscreen for correct proportions%
```

Appendix for 3.3

$10.5\ gcm \longrightarrow 342\ gcm$

$12\,380\ rpm \longrightarrow ?$

$$\text{gear ratio} = \frac{RPM_{in}}{RPM_{out}} = \frac{T_{out}}{T_{in}} = \frac{F_{out}}{F_{in}}$$

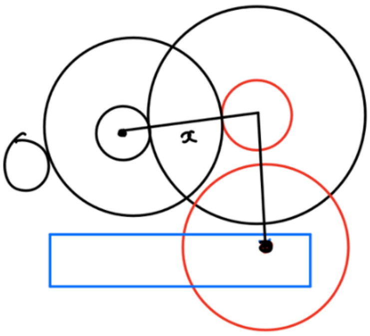

$x < y$

$2cc < s$

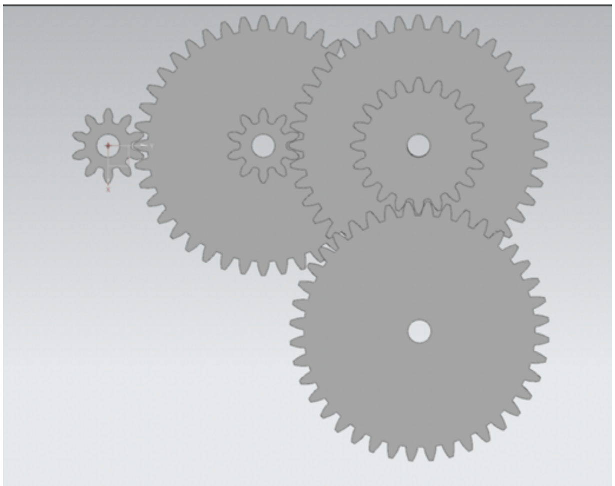

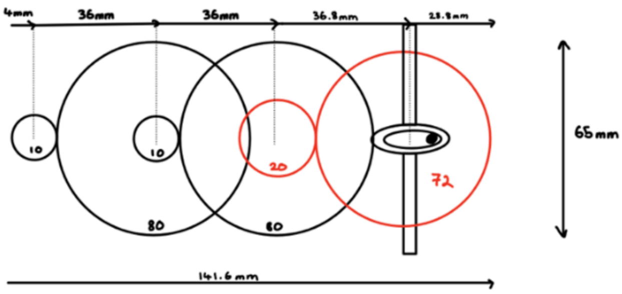

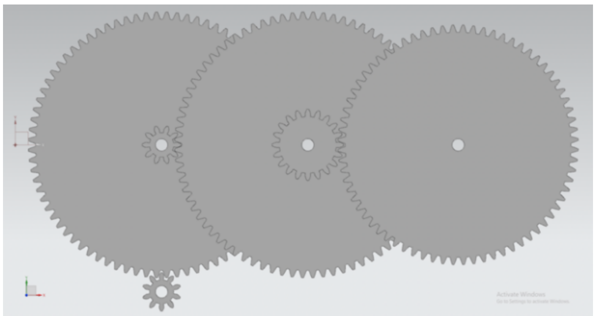

$$6500\ rpm \xrightarrow{8:1} 812.5\ rpm \xrightarrow{8:1} 101.6\ rpm \xrightarrow{3.49:1} 29.1\ rpm$$

Appendix for 4.1

Looking at inside tyre

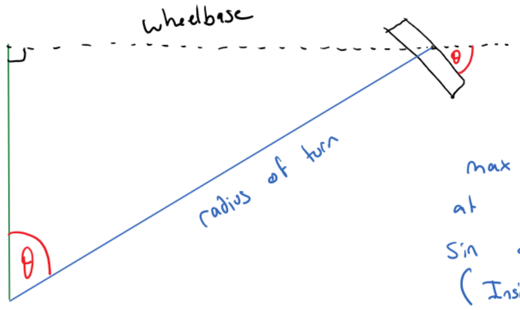

max radius of turn at highest point in Sin graph = 0.320 m (Inside wheel)

$$\sin\theta = \frac{\text{wheelbase}}{\text{radius}}$$

$$\sin\theta = \frac{0.15}{0.320} = 0.469$$

$\theta = 27.95$ So max Steering angle $= 28^\circ = 0.488$ Rad

Appendix for 4.2

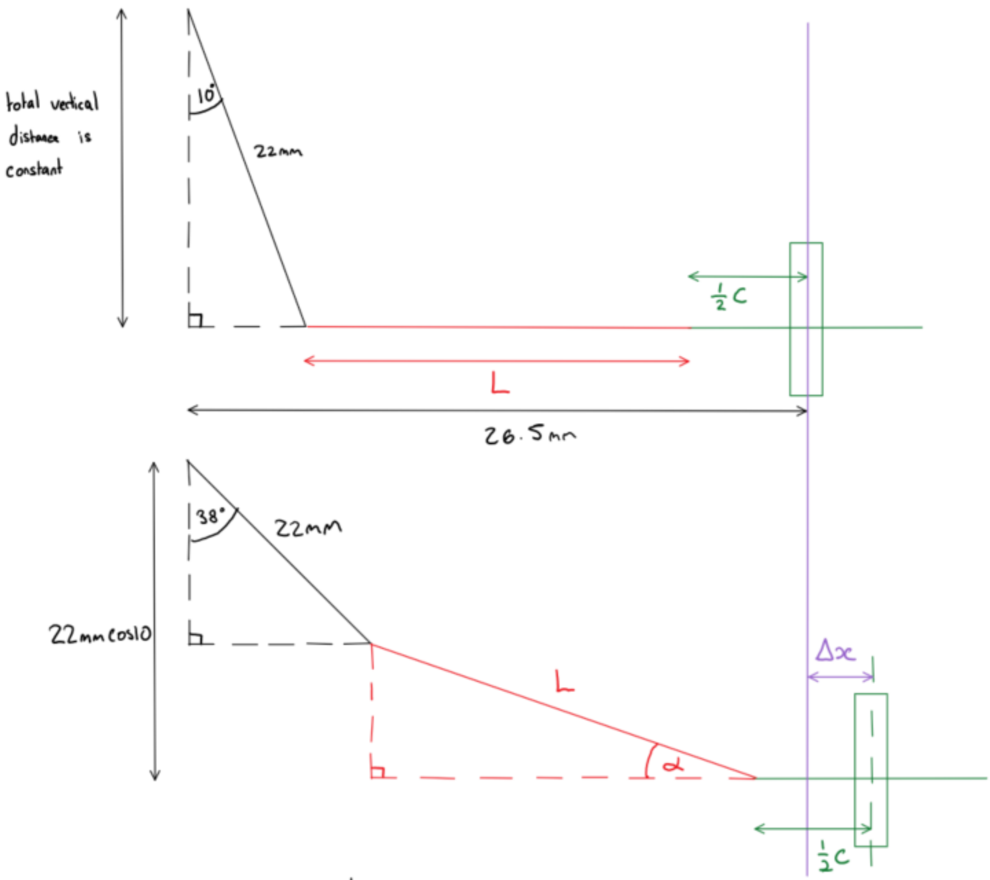

$$26.5 = \tfrac{1}{2}c + L + 22\sin 10$$

Set $c = 20$ $\quad 26.5 = 10 + L + 22\sin 10$

$$\Rightarrow L = 12.67 \quad (4\text{ s.f}) \; [\text{mm}]$$

$$22\cos 10 = 22\cos 38 + L\sin\theta$$

$$\theta = \sin^{-1}\left(\frac{22\cos 10 - 22\cos 38}{12.67}\right)$$

$$\theta = 19.97 \quad (4\text{ s.f}) \; [°]$$

$$26.5 = 22\sin 38 + L\cos\theta + \tfrac{1}{2}c - \Delta x$$

$$\Delta x = 22\sin 38 + L\cos\theta + \tfrac{1}{2}c - 26.5$$

$$\Delta x = 8.95 \quad (3\text{ s.f}) \; [\text{mm}]$$

Appendix for 4.4

Horizontal displacement for one period is 2m

at a point on graph

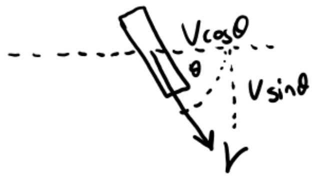

$V\cos\theta$ = horizontal velocity

$V\sin\theta$ = vertical velocity

Horizontal velocity = $V\cos\theta$ $\quad V = 1.01$

0.0.98 meter s2.12 where θ is a function of time

$\theta = kt$

in one period, θ altered from $-28°$ to $28°$

=> in radians

-0.488 to 0.488

$V = \frac{ds}{dt}$

$$\int_0^2 ds = \int V dt \qquad \theta = kt$$

$$2 = \int v\cos\theta \, dt \qquad \frac{d\theta}{dt} = k$$

$$2 = \int_{-0.488}^{0.488} \frac{V\cos\theta}{k} \, d\theta$$

$$\Rightarrow \quad 2 = \int_0^{0.488} \frac{V\cos\theta}{k} d\theta + \int_{-0.488}^{0} \frac{V\cos\theta}{k} \, d\theta$$

$$2 = \left[\frac{V\sin\theta}{k}\right]_0^{0.488} + \left[\frac{V\sin\theta}{k}\right]_{-0.488}^{0}$$

$$2 = \frac{1}{k}\left((1.01 \times 0.469) + (1.01 \times 0.469)\right)$$

$$2 = \frac{1}{k}\left(0.947\right)$$

$$k = \frac{0.947}{2} = 0.473 \text{ rad s}^{-1}$$

$$\frac{0.976}{0.473} = 2.06 \text{ s period}$$

$$\text{rpm} = \frac{60}{2.06} = 29.1$$

$$6500\text{rpm} \xrightarrow{8:1} 812.5\text{rpm} \xrightarrow{8:1} 101.6\text{rpm} \xrightarrow{3.49:1} 29.1\text{rpm}$$

Appendix for 4.6

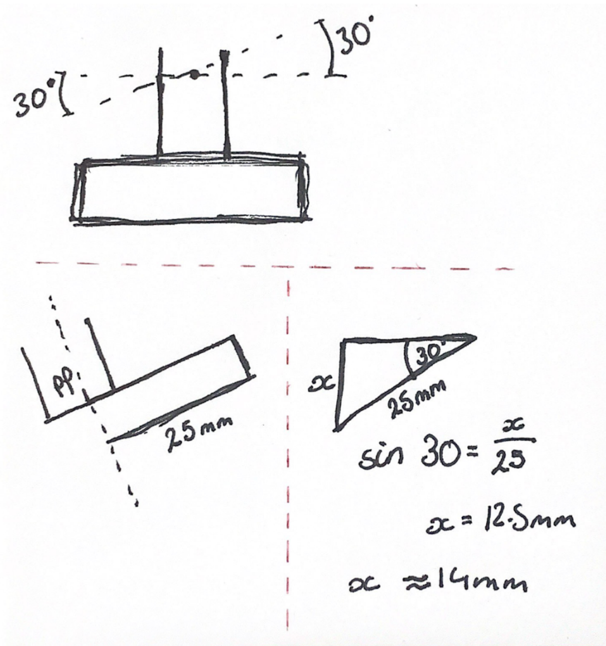

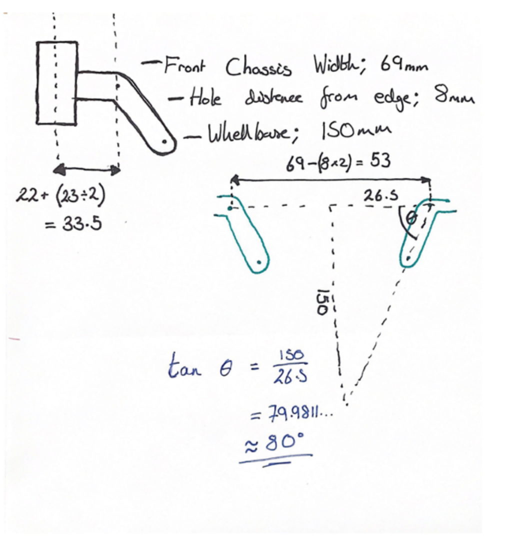

References

Colgrove, D. (2019). *Steering System for SAE Baja.* BYU ScholarsArchive.

Daniel A. Mántaras, P. L. (2004). Development and validation of a three-dimensional kinematic model for the McPherson steering and suspension mechanisms. *Mechanism and Machine Theory*, pp. 603-619.

K. Yao, Y. W. (2008). *Optimum Design and Calculation of Ackerman Steering Trapezium*. Retrieved from ieeexplore.ieee.org/abstract/document/4659693

Lynwander, P. (n.d.). *Gear Drive Systems: Design and Application*. Retrieved from https://doi.org/10.1201/9780203755075

Punnet Gautam, S. S. (2021). *Designing Variable Ackerman Steering Geomtery for Formula Student Race Car*. Retrieved from http://ischolar.info/index.php/ijaefea/article/view/209004/194335

Mass of Motor

https://docs.rs-online.com/6de0/A700000007082013.pdf

Mass of Box Section

https://www.amazon.co.uk/PVC-Square-Tube-White-20mm/dp/B01H22BGW4

Mass of Birch Ply

https://www.cutmyplastic.co.uk/wood-sheets/ply/birch/6mm/L120-W500/

Gear Systems

Lynwander, P. (1983). Gear Drive Systems: Design and Application (1st ed.). CRC Press. https://doi.org/10.1201/9780203755075